

# Turing instability in coupled nonlinear relativistic heat equations

Timoteo Carletti\* & Riccardo Muolo

*Department of Mathematics & naXys, Namur Institute for Complex Systems,  
University of Namur, rue Grafé 2, 5000 Namur, Belgium and*

*\*timoteo.carletti@unamur.be*

We hereby develop the theory of Turing instability for relativistic reaction-diffusion systems defined on complex networks. Extending the framework introduced by Cattaneo in the 40's, we remove the unphysical assumption of infinite propagation velocity holding for reaction-diffusion systems, reducing thus the gap between theory and experiments. We analytically prove that Turing instability emerges for a much broader set of conditions, e.g., once the activator diffuses faster than the inhibitor, overcoming thus the classical Turing instability framework. Analytical results are compared to direct simulations made on the FitzHugh-Nagumo model, extended to the relativistic reaction-diffusion framework with a complex network as substrate for the dynamics. We found stationary patterns, oscillatory ones, as well as a new interesting class of solutions with a stationary-like transient regime followed by an oscillatory one.

## I. INTRODUCTION

A blossoming of regular spatio-temporal patterns can be observed in Nature. These are the signature of self-organised processes where ordered structures emerge from disordered ones [1, 2]. Very often, the interaction among the microscopic units, by which the system is made of, can be modelled by means of reaction-diffusion equations that govern the deterministic evolution of the concentrations both in time and space, the latter being a regular substrate [2] or a discrete one, e.g., a complex network [3]. Spatially homogeneous equilibria of a reaction-diffusion system may undergo a symmetry breaking instability, when subjected to a heterogeneous perturbation, eventually driving the system towards a patchy, i.e., spatially heterogeneous, solution, as firstly explained by Alan Turing [4] in the 50's. Nowadays applications of the Turing instability phenomenon go well beyond the original framework of the morphogenesis and it stands for a pillar to explain self-organisation in Nature [5–7]. The conditions for the emergence of Turing patterns have been elegantly grounded on the interplay between slow diffusing activators and fast diffusing inhibitors [8]; indeed this determines a local feedback, short range production of a given species, which should be, at the same time, inhibited at long ranges. Starting from these premises, scholars have been able to extend the original Turing mechanism to non-autonomous systems, e.g., evolving domains [9, 10] or time dependent diffusion and reaction rates [11], as well as discrete substrates, e.g., lattices [12] or complex networks [13], and their generalisation, e.g., directed networks [14], multiplex networks [15] and recently to time varying networks [16, 17].

As previously observed, at the root of Turing instability there is a reaction-diffusion process which is thus grounded on a (nonlinear) “heat equation”, namely a parabolic partial differential equation (PDE). The latter is characterised by an infinite fast propagation of the initial datum along the supporting medium and thus it can accurately model the physical phenomenon only in cases of very large diffusivity,  $D \gg 1$ . To overcome this drawback, scholars have considered more realistic frameworks. In particular Cattaneo proposed in the 1948 to modify the constitutive equation (Fick's first law) by including a relaxation term with some given characteristic inertial time,  $\tau$ . Operating in this framework, Fick's second law returns a modified diffusion equation allowing also for a second derivative with respect to time [18, 19]. The resulting equation is nowadays known in the literature as the Cattaneo equation, the telegraph equation, the damped nonlinear Klein-Gordon equations or the relativistic heat equation, depending on the research field. In any case its main characteristic is to exhibit a finite propagation velocity<sup>1</sup>,  $v = \sqrt{D/\tau}$ , and moreover in the limit of arbitrarily small relaxation time,  $\tau \rightarrow 0$ , one recovers Fick's second law and thus a reaction-diffusion model with an infinite propagation velocity.

The aim of this paper is to study the conditions for the onset of Turing instability for a reaction-diffusion system defined on top of a complex network and modified according to the Cattaneo recipe, to allow for a finite propagation velocity (Section II). We thus consider two different species living on a network composed by  $n$  nodes. When species

---

<sup>1</sup> The boundedness of the propagation velocity motivates its name relativistic heat equation, observe however that no Lorentz phenomena are at play.

happen to share the same node, they interact via nonlinear functions  $f(u_i, v_i)$  and  $g(u_i, v_i)$ . On the other hand, they can diffuse across the available network links. The local currents, i.e., associated to each links, are assumed to satisfy a modified constitutive equation, Fick's first law, that includes a relaxation term with a given *inertial time*. Hence, the continuity equation, Fick's second law, allows to derive a modified local diffusion term, i.e. defined on the node. The latter, together with the reaction part, determine the hyperbolic reaction-diffusion system defined on top of a complex network, we will hereby interested in.

Our work extends the study presented in [20], realised under the simplifying hypothesis of equal inertial times for the two species, namely  $\tau_u = \tau_v$ , and assuming a continuous substrate. Indeed, we hereby assume generic inertial times for each species,  $\tau_u \neq \tau_v$ . Let observe that our results established for a discrete substrate, can be straightforwardly extended to the continuous case and thus they complete the work done in [20].

The Turing mechanism relies on the assumption of the existence of a stable homogeneous equilibrium that loses its stability once subjected to spatially heterogeneous perturbations, in presence of a diffusive term; for this reason, such process is also known as *diffusion-driven instability*. The same mechanism can be proved to hold true in the new proposed framework of the hyperbolic reaction-diffusion systems defined on top of a complex network (Section III). The dispersion relation, which ultimately signals the onset of the instability, is a function of the discrete spectrum of the Laplace matrix, namely the diffusion operator associated to the underlying network. The dispersion relation is obtained from the roots of the fourth order characteristic polynomial. To progress with the analytical understanding of the problem, we resort to the Routh-Hurwitz stability criterion [21, 32, 33], allowing to prove the (in)stability feature of a real coefficients polynomial. Let us observe that a similar approach has been recently used in [22] to deal with the emergence of patterns in hyperbolic reaction-diffusion models with cross-diffusion defined on a continuous substrate.

We have shown that the use of the inertial times strongly enlarges the parameters region for which Turing instability can emerge, even beyond the classical Turing conditions of fast inhibitor and slow activator. For generic values of the inertial times,  $\tau_u \neq \tau_v$ , we have proved that Turing instability can set up with a fast activator and slow inhibitor. As in this case classical Turing instability cannot develop and being the latter solely due to the presence of the inertial times, we propose to call them *inertia-driven Turing instability*. Of course, the proposed framework allows to prove the existence of Turing instability also for an inhibitor diffusing faster than the activator, as for the non-relativistic framework.

In the particular case where both species have the same inertial time, we have shown that the stability of the homogeneous solution is conditional to the inertial time; indeed there exists a threshold,  $\tau_{max}$ , beyond which the homogeneous equilibrium turns out to be unstable. The system exhibits thus patterns but they cannot be associated to Turing instability, even if they are indistinguishable from the latter. Moreover, the threshold  $\tau_{max}$  depends on the model parameters and there are combinations of the latter for which it is arbitrary large; stated differently, for such parameters the homogeneous equilibrium is always stable (with respect to the inertial time).

The theoretical framework hereby proposed has been complemented with a dedicated numerical analysis of the FitzHugh-Nagumo model [23–25] (see Section IV), that is a nonlinear system often used as paradigm for the study of the emergence of Turing patterns [26–29] as well as for synchronisation phenomena [30, 31]. The FitzHugh-Nagumo model has thus been extended to the framework of hyperbolic reaction-diffusion networked systems. We have numerically found stationary patterns as well as synchronised oscillatory ones. We have also found a new interesting class of solutions: after a transient time during which the system seems to settle into a stationary-like regime, it then evolves into an oscillatory stable one.

We conclude (Section V) by proposing a framework general enough to account for novel interesting results, strengthening the importance of self-organisation in nonlinear networked system and opening new directions to the applicability of the Turing instability mechanism.

## II. RELATIVISTIC REACTION-DIFFUSION SYSTEM ON NETWORKS

The aim of this section is to extend Cattaneo's idea to a discrete substrate. We will briefly show how to modify networked reaction-diffusion systems in order to allow for a finite velocity of propagation.

Let us thus consider a network made of  $n$  nodes and connected by a collection of  $m$  undirected links allowing for pairwise exchanges among nodes. Such structure can be encoded into the  $m \times n$  *incidence matrix*  $\mathbf{M}$ . Let  $e = (i, j)$  be the link connecting nodes  $i$  and  $j$ , then  $M_{ei} = 1$ ,  $M_{ej} = -1$  and  $M_{e\ell} = 0$  for all  $\ell \neq i, j$ . From this matrix we can build the *Laplace matrix*  $\mathbf{L} = -\mathbf{M}^\top \mathbf{M}$ , where  $^\top$  denotes the matrix transpose. The *Laplace matrix* is symmetric

by construction and thus it admits a set of orthonormal eigenvectors,  $\vec{\phi}^{(\alpha)}$ , and real non-positive <sup>2</sup> eigenvalues  $\Lambda^{(\alpha)}$ , for  $\alpha = 1, \dots, n$ . By construction  $\sum_j L_{ij} = 0$ , hence the largest eigenvalue is  $\Lambda^{(1)} = 0$  associated to the eigenvector  $\vec{\phi}^{(1)} = (1, \dots, 1)^\top / \sqrt{n}$ . The diagonal element  $-L_{ii}$  defines the nodes degree, say  $k_i$ , namely the number of incidents links exhibited by the  $i$ -th node; hence we can rewrite  $\mathbf{L} = \mathbf{A} - \mathbf{D}$ , where  $\mathbf{D} = \text{diag}(k_1, \dots, k_n)$  and  $\mathbf{A}$  is the *adjacency matrix*, that is  $A_{ij} = 1$  if and only if nodes  $i$  and  $j$  are connected, encoding thus the coupling network.

Let us now focus on the diffusion of a single species in the network, the generalisation to more species being a direct extension. Let  $\vec{u}(t) = (u_1(t), \dots, u_n(t))^\top$  to denote the state of the system at time  $t$ , where  $u_i(t)$  is the density of the species in node  $i$  at time  $t$ . Let  $e = (i, j)$  be a link in the network and let  $\chi_e(t)$  be the current flowing through it at time  $t$ ; then, borrowing the constitutive equation, namely Fick's first law, from the continuous framework, we can state that

$$\chi_e(t) = -D_u [u_j(t) - u_i(t)] \equiv D_u [\mathbf{M}\vec{u}(t)]_e, \quad (1)$$

that is, the current is proportional to the difference of the densities in the nodes forming the link and flowing from higher concentrations to lower ones <sup>3</sup>, being  $D_u$  the diffusion coefficient of species  $u$ . By defining the currents vector  $\vec{\chi} = (\chi_{e_1}, \dots, \chi_{e_m})^\top$ , the continuity equation can be written as

$$\frac{du_i}{dt}(t) = -[\mathbf{M}^\top \vec{\chi}(t)]_i, \quad (2)$$

namely the variation of  $u_i$  is proportional to the sum of the currents entering and exiting from node  $i$ . The classical Fick second law follows by combining the above equations:

$$\frac{d\vec{u}}{dt}(t) = -\mathbf{M}^\top \vec{\chi} = -D_u \mathbf{M}^\top \mathbf{M} \vec{u} = D_u \mathbf{L} \vec{u}, \quad (3)$$

where we can realise [12, 13] that  $\mathbf{L}$  replaces the second order differential operator used in the continuous substrate case and thus the model given by (3) exhibits infinite propagation velocity.

To overcome this problem we modify, as Cattaneo did, the constitutive equation (1) by introducing a relaxation factor with some characteristic inertial time  $\tau_u$ , namely

$$\chi_e(t) + \tau_u \frac{d\chi_e}{dt}(t) = -D_u [\mathbf{M}\vec{u}(t)]_e. \quad (4)$$

Combining this equation with the continuity equation (2) allows to obtain

$$\begin{aligned} \frac{d\vec{u}}{dt}(t) &= -\mathbf{M}^\top \vec{\chi} = -\mathbf{M}^\top \left[ -\tau_u \frac{d\vec{\chi}}{dt} - D_u \mathbf{M} \vec{u}(t) \right] = \tau_u \frac{d\mathbf{M}^\top \vec{\chi}}{dt} + D_u \mathbf{M}^\top \mathbf{M} \vec{u}(t) \\ &= -\tau_u \frac{d^2 \vec{u}}{dt^2} + D_u \mathbf{L} \vec{u}(t), \end{aligned} \quad (5)$$

eventually providing the generalised Cattaneo equation defined on networks

$$\frac{d\vec{u}}{dt}(t) + \tau_u \frac{d^2 \vec{u}}{dt^2}(t) = D_u \mathbf{L} \vec{u}(t). \quad (6)$$

Consider now two different species populating a network composed by  $n$  nodes and let us denote by  $u_i$  and  $v_i$ ,  $i = 1, \dots, n$ , their respective concentrations on node  $i$ . When species happen to share the same node, they interact via nonlinear functions  $f(u_i, v_i)$  and  $g(u_i, v_i)$ . On the other hand, they can diffuse across the available network links accordingly to the modified Cattaneo equation (6). The model can hence be mathematically cast in the form

$$\begin{aligned} \frac{du_i}{dt} + \tau_u \frac{d^2 u_i}{dt^2} &= f(u_i, v_i) + D_u \sum_{j=1}^n L_{ij} u_j \\ \frac{dv_i}{dt} + \tau_v \frac{d^2 v_i}{dt^2} &= g(u_i, v_i) + D_v \sum_{j=1}^n L_{ij} v_j, \end{aligned} \quad (7)$$

<sup>2</sup> The matrix  $\mathbf{L}$  is non-negative definite. Indeed let  $\vec{\phi}^{(\alpha)}$  be any orthonormal eigenvector, then  $(\vec{\phi}^{(\alpha)}, \mathbf{L} \vec{\phi}^{(\alpha)}) = \Lambda^{(\alpha)}$  and at the same time  $(\vec{\phi}^{(\alpha)}, \mathbf{L} \vec{\phi}^{(\alpha)}) = -(\vec{\phi}^{(\alpha)}, \mathbf{M}^\top \mathbf{M} \vec{\phi}^{(\alpha)}) = -(\mathbf{M} \vec{\phi}^{(\alpha)}, \mathbf{M} \vec{\phi}^{(\alpha)}) = -\|\mathbf{M} \vec{\phi}^{(\alpha)}\|^2 \leq 0$ .

<sup>3</sup> Let us observe that, despite the different sign in front of Eq. (1), the latter is the analogous of the Fick's first law in the continuous setting: the current flows from regions of higher concentration to regions of lower one. Indeed once we fix the link "ordering" as  $e = (i, j)$ , then the current  $\chi_e$  will be positive, i.e. respecting the link ordering if  $u_i > u_j$ , while the current will be negative, i.e. opposite to the link order if  $u_i < u_j$ .

where  $D_u$  (resp.  $D_v$ ) is the diffusion coefficients of species  $u$  (resp.  $v$ ) and  $\tau_u$  (resp.  $\tau_v$ ) the inertial time for species  $u$  (resp.  $v$ ).

### III. TURING INSTABILITY IN RELATIVISTIC REACTION-DIFFUSION SYSTEMS DEFINED ON NETWORK

The Turing mechanism is the result of a diffusion-driven instability, namely an homogeneous stable equilibrium of the reaction-diffusion system turns out to be unstable, with respect to inhomogeneous spatial perturbations, once the diffusion is at play. The aim of this section is to determine the conditions for such instability to develop in the relativistic reaction-diffusion systems defined on networks given by Eq. (7).

Let us hence assume there exists an homogeneous solution of (7), that is  $u_i(t) = u_0$  and  $v_i(t) = v_0$  for all  $i = 1, \dots, n$  and  $t > 0$ . Namely  $u_0$  and  $v_0$  should satisfy  $f(u_0, v_0) = g(u_0, v_0) = 0$ . Let us denote by  $\delta u_i(t) = u_i(t) - u_0$  and  $\delta v_i(t) = v_i(t) - v_0$  the perturbations from the homogeneous solution. In order to determine the time evolution of the latter, we use (7), keeping only the first order terms in the perturbation (the latter assumed to be small). We thus obtain

$$\begin{aligned} \frac{d\delta u_i}{dt} + \tau_u \frac{d^2 \delta u_i}{dt^2} &= \partial_u f \delta u_i + \partial_v f \delta v_i + D_u \sum_{j=1}^n L_{ij} \delta u_j \\ \frac{d\delta v_i}{dt} + \tau_v \frac{d^2 \delta v_i}{dt^2} &= \partial_u g \delta u_i + \partial_v g \delta v_i + D_v \sum_{j=1}^n L_{ij} \delta v_j, \end{aligned} \quad (8)$$

where we employed the fact that  $\sum_j L_{ij} = 0$  to simplify the terms  $\sum_j L_{ij}(\delta u_j(t) + u_0)$  and  $\sum_j L_{ij}(\delta v_j(t) + v_0)$ . Let us also stress that throughout the rest of the section the partial derivatives, i.e.,  $\partial_u f \equiv \partial f / \partial u$  and similarly for the other ones, are evaluated at the homogeneous equilibrium  $(u_0, v_0)$ .

To progress with the analytical understanding, we develop the perturbations on the eigenbasis of the Laplace matrix  $\delta u_i(t) = \sum_\alpha \hat{u}_\alpha(t) \phi_i^{(\alpha)}$  and  $\delta v_i(t) = \sum_\alpha \hat{v}_\alpha(t) \phi_i^{(\alpha)}$ . Inserting the latter into Eq. (8) we obtain the equation ruling the evolution of the modes  $\hat{u}_\alpha(t)$  and  $\hat{v}_\alpha(t)$

$$\begin{aligned} \frac{d\hat{u}_\alpha}{dt}(t) + \tau_u \frac{d^2 \hat{u}_\alpha}{dt^2}(t) &= \partial_u f \hat{u}_\alpha(t) + \partial_v f \hat{v}_\alpha(t) + D_u \Lambda^{(\alpha)} \hat{u}_\alpha(t) \\ \frac{d\hat{v}_\alpha}{dt}(t) + \tau_v \frac{d^2 \hat{v}_\alpha}{dt^2}(t) &= \partial_u g \hat{u}_\alpha(t) + \partial_v g \hat{v}_\alpha(t) + D_v \Lambda^{(\alpha)} \hat{v}_\alpha(t), \end{aligned} \quad (9)$$

namely we end up with  $n$  linear  $2 \times 2$  systems instead of the initial  $2n \times 2n$  one. We further hypothesise  $\hat{u}_\alpha(t) \sim e^{\lambda_\alpha t}$  and  $\hat{v}_\alpha(t) \sim e^{\lambda_\alpha t}$ , and to ensure the existence of a non trivial solution we eventually obtain that the linear growth rate  $\lambda_\alpha$  should solve

$$\det \begin{pmatrix} \lambda_\alpha + \tau_u \lambda_\alpha^2 - \partial_u f - \Lambda^{(\alpha)} D_u & -\partial_v f \\ -\partial_u g & \lambda_\alpha + \tau_v \lambda_\alpha^2 - \partial_v g - \Lambda^{(\alpha)} D_v \end{pmatrix} = 0 \Leftrightarrow p_\alpha(\lambda_\alpha) = 0, \quad (10)$$

where the fourth degree polynomial is defined by

$$p_\alpha(\lambda) = a\lambda^4 + b\lambda^3 + c_\alpha\lambda^2 + d_\alpha\lambda + e_\alpha, \quad (11)$$

whose coefficients are given by

$$a = \tau_u \tau_v, \quad b = (\tau_u + \tau_v) \quad (12)$$

$$c_\alpha = 1 - \tau_u \partial_v g - \tau_v \partial_u f - \Lambda^{(\alpha)} (\tau_u D_v + \tau_v D_u) \quad (13)$$

$$d_\alpha = -\text{tr}(J_0) - \Lambda^{(\alpha)} (D_v + D_u) \quad (14)$$

$$e_\alpha = \det(J_0) + (D_v \partial_u f + D_u \partial_v g) \Lambda^{(\alpha)} + D_u D_v \left( \Lambda^{(\alpha)} \right)^2, \quad (15)$$

being  $J_0 = \begin{pmatrix} \partial_u f & \partial_v f \\ \partial_u g & \partial_v g \end{pmatrix}$  the Jacobian of the aspatial reaction system evaluated at the homogeneous equilibrium  $(u_0, v_0)$ ,  $\text{tr}(J_0) = \partial_u f + \partial_v g$  its trace and  $\det(J_0) = \partial_u f \partial_v g - \partial_v f \partial_u g$  its determinant. Notice that the coefficients  $a$  and  $b$  are positive and do not depend on the index  $\alpha$ .

Turing instability arises if the homogeneous equilibrium  $(u_0, v_0)$  is stable, namely if the four roots of the polynomial  $p_1(\lambda)$  all have negative real part <sup>4</sup>, while there exists at least one  $\alpha > 1$  for which the polynomial  $p_\alpha(\lambda)$  does admit at least one root with positive real part. The root with the largest real part <sup>5</sup>, seen as a function of  $\Lambda^{(\alpha)}$ , is called in the literature the *dispersion relation*,  $\lambda_\alpha := \max_{i=1,\dots,4} \Re \lambda_i(\Lambda^{(\alpha)})$ . Turing instability is thus equivalent to require  $\lambda_1 < 0$  and  $\lambda_\alpha > 0$  for some  $\alpha > 1$ .

To prove the existence of Turing instability for the system (7) we shall rely on the Routh-Hurwitz criterion [21, 32, 33], providing necessary and sufficient conditions to prove that  $p_1$  is stable <sup>6</sup> while  $p_\alpha$  is unstable for some  $\alpha > 1$ .

**Remark** (*Connection with the relativistic reaction-diffusion system defined on a continuous substrate*) As already remarked, the Laplace matrix  $\mathbf{L}$  in Eq. (7) takes the place of the second order differential operator  $\Delta = \sum_i \partial_{x_i}$ . After linearising the resulting PDE system about the homogeneous equilibrium, the use of the periodic boundary conditions and the Fourier series, is equivalent to project the linear system onto the eigenfunctions of  $\Delta$ , that is  $e^{ikx}$  (for  $k \in \mathbb{Z}$ , in the case of a 1 dimensional spatial domain), whose eigenvalues are  $-k^2$ . Proceeding in this way, one can determine a polynomial similar to the one given in (11), where we have to replace  $\Lambda^{(\alpha)}$  by  $-k^2$ . Our results based on the assumption of different inertial times,  $\tau_u \neq \tau_v$ , can thus be straightforwardly extended to the PDE setting, i.e., assuming a continuous substrate. However, let us observe that now the spectrum of  $\mathbf{L}$  is discrete, which may introduce finite size effects.

### A. Conditions for the stability of $p_1$

The aim of this section is to introduce the conditions for the linear stability of the homogeneous solution of (7). As already noticed, the coefficients  $a = \tau_u \tau_v$  and  $b = \tau_u + \tau_v$  are positive, hence the necessary and sufficient conditions (see Appendix A) to ensure the stability of  $p_1$  are given by:

$$1 - \tau_u \partial_v g - \tau_v \partial_u f > 0 \quad (16)$$

$$\text{tr}(J_0) = \partial_u f + \partial_v g < 0 \quad (17)$$

$$\det(J_0) = \partial_u f \partial_v g - \partial_v f \partial_u g > 0 \quad (18)$$

$$(\tau_u + \tau_v)(1 - \tau_u \partial_v g - \tau_v \partial_u f) + \tau_u \tau_v \text{tr}(J_0) > 0 \quad (19)$$

$$-\text{tr}(J_0) [(\tau_u + \tau_v)(1 - \tau_u \partial_v g - \tau_v \partial_u f) + \tau_u \tau_v \text{tr}(J_0)] - (\tau_u + \tau_v)^2 \det(J_0) > 0, \quad (20)$$

Before proceeding in our analysis, let us consider a special but relevant case, namely  $\tau_u = \tau_v = \tau$ . Assuming Eq. (17) to hold true, then Eqs. (16) and (19) easily follow. Moreover, if  $4 \det(J_0) < (\text{tr}(J_0))^2$ , then Eq. (20) is always satisfied, while if  $4 \det(J_0) > (\text{tr}(J_0))^2$ , the following upper bound for  $\tau$  is obtained to satisfy (20):

$$\tau < \tau_{max} = \frac{-2\text{tr}(J_0)}{[4 \det(J_0) - (\text{tr}(J_0))^2]}. \quad (21)$$

This last results will be important in the following, because it states that the stability of the homogeneous equilibrium depends on  $\tau$  (see panel b) in Fig. 1); more importantly, if  $\tau$  is large enough, the system (7) exhibits patterns, however they are not emerging from Turing instability but from the instability of the homogeneous equilibrium.

### B. Conditions for the instability of $p_\alpha$

Using again the Routh-Hurwitz criterion we can prove the existence of (at least) a  $\alpha > 1$  for which  $p_\alpha$  is unstable conditioned on the stability of  $p_1$ .

Observe again that the coefficients  $a$  and  $b$  are positive. Moreover, by assuming Eqs. (16) and (17) to hold true and by recalling that  $-\Lambda^{(\alpha)} > 0$  for all  $\alpha > 1$ , then  $c_\alpha > 0$  and  $d_\alpha > 0$  (see Eqs. (13) and (14)). In conclusion the

<sup>4</sup> Inspecting Eq. (9) it is clear that the  $\Lambda^{(1)} = 0$  eigenvalue represents the behaviour of the aspatial system.

<sup>5</sup> The largest imaginary parts of the four roots associated with a positive real part, will be denoted by  $\rho_\alpha := \max_{i=1,\dots,4} \{\Im \lambda_i(\Lambda^{(\alpha)}) : \lambda_\alpha > 0\}$ .

<sup>6</sup> Let us recall that, borrowed from the theory of the linear stability of dynamical systems, a polynomial is stable if and only if all its roots have negative real part, while a polynomial is said to be unstable if there exists at least one root with positive real part.

unique coefficient of  $p_\alpha$  that can be negative is  $e_\alpha$ . Hence (see Appendix A) instability can arise if one of the following couples of conditions is verified:

$$\begin{aligned} B &:= -(\tau_u + \tau_v)(D_u + D_v)(1 - \tau_u \partial_v g - \tau_v \partial_u f) + (\tau_u + \tau_v) \text{tr}(J_0)(\tau_u D_v + \tau_v D_u) \\ &\quad - 2 \text{tr}(J_0)(D_u + D_v) \tau_u \tau_v - (\tau_u + \tau_v)^2 (D_v \partial_u f + D_u \partial_v g) > 0 \end{aligned} \quad (22)$$

$$\begin{aligned} B^2 &- 4(D_v \tau_u - D_u \tau_v)^2 \left[ -\text{tr}(J_0)(\tau_u + \tau_v)(1 - \tau_u \partial_v g - \tau_v \partial_u f) \right. \\ &\quad \left. - \tau_u \tau_v (\text{tr}(J_0))^2 - (\tau_u + \tau_v)^2 \det(J_0) \right] > 0, \end{aligned} \quad (23)$$

or

$$D_u \partial_v g + D_v \partial_u f > 0 \quad (24)$$

$$(D_u \partial_v g + D_v \partial_u f)^2 - 4 D_u D_v \det(J_0) > 0, \quad (25)$$

Let us observe that Eqs. (24) and (25) do not depend on  $\tau_u$  and  $\tau_v$  and are indeed the same conditions one imposes to obtain Turing instability [13]. In particular, they require  $D_v > D_u$ . However, Eqs. (22) and (23) do not require such condition on the diffusivities, implying that the hypothesis of a finite propagation velocity allows to enlarge the parameters region for which Turing instability arises.

Let us thus consider the case  $D_u = D_v = D$ . As already observed Eq. (24) cannot be satisfied being the  $\text{tr}(J_0) < 0$  by Eq. (17), thus this cannot be a path towards Turing instability. On the other hand, let us reorganise terms and rewrite condition (22) as follows

$$B|_{D_u=D_v=D} = -2D [\tau_u + \tau_v + (\tau_u^2 - \tau_v^2) \partial_u f + \tau_u (\tau_v - \tau_u) \text{tr}(J_0)],$$

and observe that if  $\tau_u \geq \tau_v$  then  $B|_{D_u=D_v=D} < 0$ . Indeed,  $\partial_u f > 0$ , being  $u$  the activator species, and  $\text{tr}(J_0) < 0$  by the stability assumption on  $p_1(\lambda)$ ; hence the term in brackets on the right hand side is the sum of three positive terms, from which the claim follows. On the contrary, if  $\tau_u < \tau_v$ , then  $B|_{D_u=D_v=D} > 0$  provided

$$-\text{tr}(J_0) > \frac{\tau_u + \tau_v}{\tau_u(\tau_v - \tau_u)} - \frac{\tau_u + \tau_v}{\tau_u} \partial_u f.$$

Finally, condition (23) no longer depends on  $D$  and can thus be verified by a suitable choice of the remaining parameters.

In conclusion, we can have Turing instability also in the case of equal diffusivities,  $D_u = D_v$ , provided the inhibitor has a larger inertial time than the activator,  $\tau_v > \tau_u$ .

Let us conclude this section by considering again the case  $\tau_u = \tau_v = \tau$ . Because of the previous analysis we have to assume  $D_u \neq D_v$ , because otherwise no Turing instability can develop. Then Eq. (22) simplifies into

$$B|_{\tau_u=\tau_v=\tau} = -2\tau [(D_u + D_v) + \tau(D_v - D_u)(\partial_u f - \partial_v g)].$$

Being  $v$  the inhibitor species we have  $\partial_v g < 0$ , hence, if  $D_v > D_u$ , we can conclude that the term in brackets on the right hand side is the sum of positive terms and thus  $B|_{\tau_u=\tau_v=\tau} < 0$ . On the other hand, if  $D_v < D_u$ , we can have  $B|_{\tau_u=\tau_v=\tau} > 0$  provided that

$$\tau > \frac{D_u + D_v}{D_u - D_v} \frac{1}{\partial_u f - \partial_v g}.$$

Finally, the remaining condition (23) can be rewritten as

$$4\tau^2 [(D_u + D_v)^2 + 2D_u D_v \text{tr}(J_0) - 4\tau^2 (D_v - D_u)^2 \det(J_0)] > 0,$$

and a straightforward computation allows to show that it is satisfied if

$$\tau > \frac{D_u D_v \text{tr}(J_0) + \sqrt{[D_u D_v \text{tr}(J_0)]^2 + 4(D_v^2 - D_u^2)^2 \det(J_0)}}{4(D_v - D_u)^2 \det(J_0)}.$$

Let us stress that in this setting,  $D_v < D_u$ , the conditions (22) and (23) cannot be satisfied, hence the emergence of Turing instability is solely due to the finite propagation velocity and imposes a lower bound on the inertial time.

#### IV. THE FITZHUGH-NAGUMO MODEL

The aim of this section is to present an application of the theory hereby developed. For the sake of definitiveness, we decided to use the FitzHugh-Nagumo model [23–25], but of course our results go beyond the chosen model. The FitzHugh-Nagumo model (for short *FHN*) is a paradigmatic nonlinear system already used in the literature to study the emergence of Turing patterns [26–29] as well as synchronisation phenomena [30, 31]. Our choice relies also on the observation that such model has been conceived in the framework of neuroscience as a schematisation of an electric impulse propagating through an axon. For this reason, we believe that it would make a suitable setting to account for a finite velocity propagation of signals and it could be interesting for future applications.

The *FHN* model can be described by the system of ODE

$$\begin{aligned}\frac{du}{dt} &= \mu u - u^3 - v \\ \frac{dv}{dt} &= \gamma(u - \beta v).\end{aligned}\tag{26}$$

where the parameters  $\mu$ ,  $\gamma$  and  $\beta$  are assumed to be positive. We will hereby focus on its behaviour close to the fixed point  $(u_0, v_0) = (0, 0)$ . The linear stability analysis ensures stability of the latter under the conditions  $\mu < \gamma\beta$  and  $\mu\beta < 1$  (see panel a) in Fig. 1). Let us observe that, once such conditions are not met, the system undergoes a subcritical Hopf-Antonov bifurcation [34]: the equilibrium point becomes unstable giving birth to a limit cycle solution. In this study we will limit ourselves to the former case, leaving the oscillating case for a future work.

Consider now  $n$  identical copies of the FitzHugh-Nagumo model (26) interacting each other with a diffusive-like coupling and assume to work in the Cattaneo framework presented in Section II. The resulting model can thus be written as

$$\begin{aligned}\frac{du_i}{dt} + \tau_u \frac{d^2 u_i}{dt^2} &= \mu u_i - u_i^3 - v_i + D_u \sum_{j=1}^n L_{ij} u_j \\ \frac{dv_i}{dt} + \tau_v \frac{d^2 v_i}{dt^2} &= \gamma(u_i - \beta v_i) + D_v \sum_{j=1}^n L_{ij} v_j,\end{aligned}\tag{27}$$

where  $D_u$  (resp.  $D_v$ ) is the diffusion coefficients of species  $u$  (reps.  $v$ ) and  $\tau_u$  (resp.  $\tau_v$ ) the inertial time for species  $u$  (resp.  $v$ ). The matrix  $\mathbf{L}$  is the Laplace matrix describing the diffusive coupling among the FitzHugh-Nagumo systems.

**Remark** (*About the network substrate*) The possible onset of Turing instability depends both on the dynamical system as well as the network substrate via the eigenvalues  $\Lambda^{(\alpha)}$  of the associated Laplace matrix,  $\mathbf{L}$ . As previously stated, a discrete topology may affect the dynamics due to finite size effects. However, a deep study of such impact on Turing instability goes beyond the scope of this paper. Therefore, for the sake of definitiveness, we decided to use an Erdős-Rényi random graph [35] made of  $n$  nodes and with a probability  $p \in (0, 1)$  to have a link between any couple of nodes. In the following we fixed  $n = 30$  and  $p = 0.1$  and we also checked that the resulting network is connected.

In the rest of this Section we will present our analysis about the emergence of Turing instability in the relativistic *FHN* defined on networks (27). Let us start by determining the parameters region associated to a stable homogeneous equilibrium,  $(u_0, v_0) = (0, 0)$ . The panel a) of Fig. 1 represents the classical case where we assume an infinite propagation velocity, namely  $\tau_u = \tau_v = 0$ . The stability region (black) is delimited by the conditions  $\mu < \gamma\beta$  (red line) and  $\mu\beta < 1$  (yellow line). In panel b) we report the case of equal inertial times,  $\tau_u = \tau_v = 1$ ; we can observe that the stability region (black and shades of grey) is contained in the previous one, being delimited by the same conditions and in addition by Eq. (20) (blue line). As previously observed, the stability of the homogeneous solution depends on the value of  $\tau_u = \tau_v = \tau$ , meaning that the equilibrium loses its stability if the inertial time is too large, as shown by Eq. (21). The grey shaded region in panel b) has thus been coloured according to  $\ln \tau_{max}$ : smaller values are associated to lighter shades of grey. On the contrary, in the black region any positive value of  $\tau$  returns a stable homogeneous equilibrium (being  $\tau_{max} = \infty$ ). In the remaining panels of Fig. 1 we considered different inertial times,  $\tau_u = 5$  and  $\tau_v = 1$  in panel c), and  $\tau_u = 1$  and  $\tau_v = 5$  in panel d). The stability region (black) is delimited by the same lines as before, with the exception of the case  $\tau_u < \tau_v$ , where an extra condition needs to be considered, i.e., Eq. (19) (green line).

We are now able to study the emergence of Turing instability under the assumption  $\tau_u = \tau_v$ . In the panel a) of Fig. 2 we report the region (black) in the parameters space allowing for classical Turing instability to arise for a choice of the diffusivities  $D_u < D_v$ . Such region is contained in the one associated to a stable homogeneous solution and it is now also bounded by the conditions  $D_v \partial_u f + D_u \partial_v g = 0$  (dashed blue line) and  $(D_u \partial_v g + D_v \partial_u f)^2 - 4D_u D_v \det(J_0) = 0$

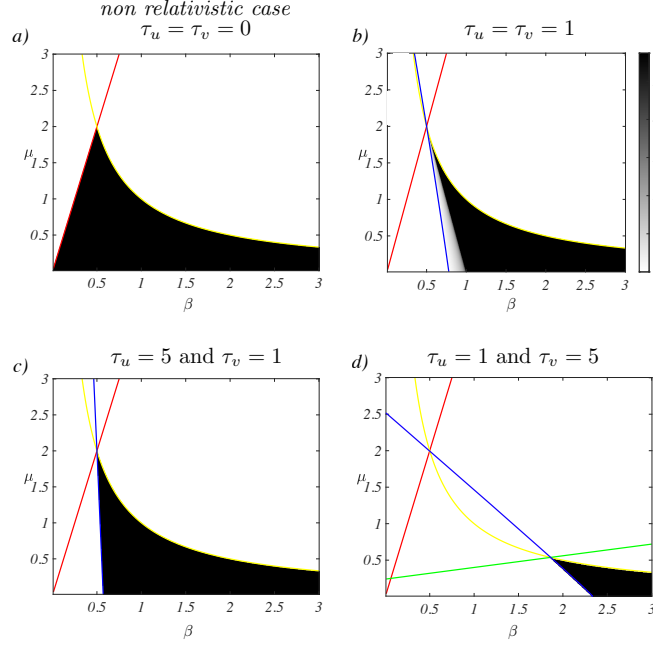


FIG. 1: **Parameters region associated to the stability of the homogeneous solution for the *FHN* model.** For a fixed value of  $\gamma = 4$ , we study the stability of the homogeneous equilibrium  $(u_i, v_i) = (0, 0)$ ,  $i = 1, \dots, n$ , as a function of  $\beta$  and  $\mu$ : the black regions denote stability while white ones instability. Panel a) corresponds to the classical setting, i.e.,  $\tau_u = \tau_v = 0$ , the remaining panels are associated to positive values of the inertial times,  $\tau_u = \tau_v = 1$  (panel b)),  $\tau_u = 5$  and  $\tau_v = 1$  (panel c)) and  $\tau_u = 1$  and  $\tau_v = 5$  (panel d)). In all the panels the red line denotes the condition  $\text{tr}(J_0) = 0$ , while  $\det(J_0) = 0$  is represented by the yellow one; these two lines determine the boundary of the stability region in the classical setting. Such region is shrunk in the case of positive inertial times because of the additional constraints, Eq. (19) (green line) and Eq. (20) (blue one). The grey shaded region in panel b), coloured according to  $\ln \tau_{max}$ , is associated to a stability of the homogenous equilibrium constrained to a bound on  $\tau$ , see Eq. (21), while in the black region any positive value of  $\tau$  is admissible.

(dashed red line). The same values of the parameters are used in panel b) assuming now the inertial times to be positive,  $\tau_u = \tau_v = 1$ ; the Turing region (black and shades of grey) is smaller, as it is also delimited by the condition Eq. (20) (blue line). Once again, the shades of grey represent the values of  $\ln \tau_{max}$  to ensure the stability of the homogeneous solution (see Eq. (21)). Finally in panel c) we report the analysis of a setting for which classical Turing instability can never emerge because the inhibitor diffuses slower than the activator,  $D_u = 2.2 > D_v = 0.2$ : this is thus an *inertia-driven instability*. The Turing region (black and shades of grey) is now delimited also by the condition Eq. (23), where again the shades of grey represent the values of  $\ln \tau_{max}$ .

The impact of  $\tau_{max}$  can be appreciated in Fig. 3 where we report the *dispersion relation*,  $\lambda_\alpha$ , as a function of  $\Lambda^{(\alpha)}$ , the eigenvalues of the Laplace matrix,  $\mathbf{L}$ . In panel a) we show the dispersion relation for the choice  $\tau_u = \tau_v = 1$  and  $(\beta, \mu) = (0.8, 1.0)$ , lying in the Turing instability region (yellow star in the panel c) of Fig. 2). We can observe that the homogeneous equilibrium is stable (the relation dispersion is negative for  $\Lambda^{(1)} = 0$ ) but it turns out to be unstable under heterogeneous perturbations (there exist  $\alpha > 1$  (red dots) for which  $\lambda_\alpha > 0$ ) and synchronised oscillatory patterns emerge (data not shown). Panel b) ( $\tau_u = \tau_v = 2.2$  and  $(\beta, \mu) = (0.7, 1.0)$ , red triangle in the panel c) of Fig. 2) corresponds to a similar behaviour, being the parameters still in the Turing region but conditioned to the value of  $\tau_{max}$ ; the dispersion relation assumes positive values but the homogeneous equilibrium is weakly stable, the relation dispersion is negative but very close to 0 for  $\Lambda^{(1)} = 0$ , being  $\tau_u = \tau_v = 2.2$  close to  $\tau_{max} \sim 2.31$ . In panel c) we used the same parameters  $(\beta, \mu)$  but we increased the inertial times beyond the critical values,  $\tau_u = \tau_v = 3.5 > \tau_{max}$ , and indeed the homogeneous equilibrium is unstable, the dispersion relation is positive for  $\Lambda^{(1)} = 0$ . Again synchronised oscillatory patterns emerge (data not shown), they are indistinguishable from the ones one can obtain from the setting presented in panels a) and b) but they are not the result of Turing instability.

We can now consider the more general case of different inertial times and show the onset of Turing instability for a choice of the diffusivities that cannot allow for the classical Turing phenomenon, notably because the activator can diffuse faster than the inhibitor. For this reason we hereby name such new phenomena as *inertia-driven Turing*



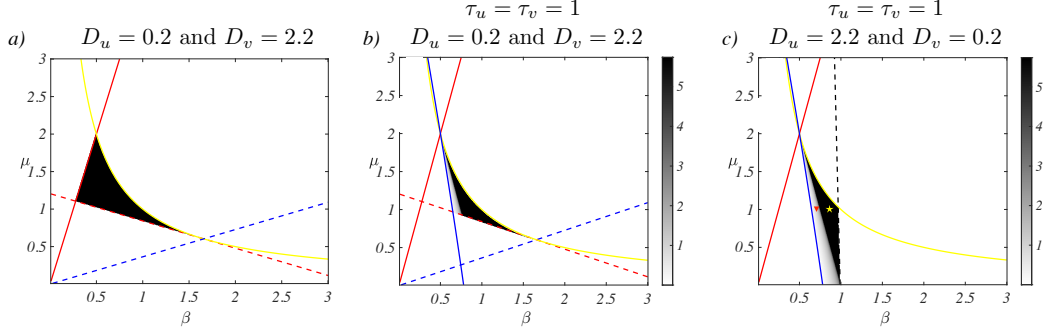


FIG. 2: **Parameters region associated to Turing instability for the *FHN* model,  $\tau_u = \tau_v$ .** For a fixed value of  $\gamma = 4$ , we study the onset of Turing instability (black regions) close to the homogeneous equilibrium  $(u_i, v_i) = (0, 0)$ ,  $i = 1, \dots, n$ , as a function of  $\beta$  and  $\mu$ . Panel a) corresponds to the classical setting, i.e.,  $\tau_u = \tau_v = 0$ , the remaining panels are associated to positive values of the inertial times,  $\tau_u = \tau_v = 1$ . In panels a) and b) the diffusivities have been set equal to  $D_u = 0.2$  and  $D_v = 2.2$ , namely the inhibitor diffuses faster than the activator. Panel c) present a completely new setting where Turing instability can develop even for a slower inhibitor,  $D_u = 2.2$  and  $D_v = 0.2$ . In all the panels the red line denotes the condition  $\text{tr}(J_0) = 0$ , while  $\det(J_0) = 0$  is represented by the yellow one. In panels a) and b), the dashed blue line represents the condition  $D_v \partial_u f + D_u \partial_v g = 0$  (Eq. (24)), while the dashed red line the condition  $(D_u \partial_v g + D_v \partial_u f)^2 - 4 D_u D_v \det(J_0) = 0$  (Eq. (25)). Together with the blue line in panel b) corresponding to Eq. (20), these lines delimitate the parameters region allowing for Turing instability in the case  $D_u < D_v$ . In panel c), corresponding to  $D_u > D_v$ , a similar parameters region is bounded by the same blue line but also by the dashed black line, namely Eq. (23). The grey shaded region in panels b) and c), coloured according to  $\ln \tau_{max}$ , is associated to a stability of the homogeneous equilibrium constrained to a bound on  $\tau$ , see Eq. (21), while in the black region any positive value of  $\tau$  is admissible.

*instability.*

In Fig. 4 we report the region (black) in the parameters space  $(\beta, \mu)$  allowing for Turing instability under the assumptions  $\tau_u \neq \tau_v$  and  $D_u \geq D_v$ . Such region is contained in the region associated to a stable homogeneous solution (see panels c) and d) of Fig. 1) and delimited in addition by the conditions (19) (green line), (20) (magenta line) and (23) (dashed black line). We can observe that for all the choices of the inertial times and diffusion constants ( $\tau_u = 5$ ,  $\tau_v = 1$ ,  $D_u = 2.2$  and  $D_v = 0.2$  panel a),  $\tau_u = 1$ ,  $\tau_v = 5$ ,  $D_u = 2.2$  and  $D_v = 0.2$  panel b) and  $\tau_u = 1$ ,  $\tau_v = 5$ ,  $D_u = D_v = 2.2$  panel c)) there are always parameters  $(\beta, \mu)$  allowing Turing instability to occur.

In Fig. 5 we report two generic dispersion relations for the inertia-driven setting. In both cases we can appreciate the fact that the aspatial solution is stable, indeed  $\lambda_1 < 0$ , while there are  $\alpha > 1$  (red dots) for which  $\lambda_\alpha > 0$ , testifying the instability of such equilibrium once subjected to heterogeneous perturbations and resulting into synchronised oscillatory patterns (data not shown).

The results reported in Fig. 6 correspond to a parameters setting for which classical Turing instability, i.e.,  $\tau_u = \tau_v = 0$ , could emerge because the inhibitor diffuses faster than the activator. The resulting patterns are however quite different in the present case,  $\tau_u > 0$  and  $\tau_v > 0$  (see Fig. 7). In the panel a) we clearly show that Turing instability is at play; indeed, the aspatial equilibrium is stable,  $\lambda_1 < 0$ , and there are modes  $\alpha > 1$  for which the dispersion relation is positive,  $\lambda_\alpha > 0$ ; moreover, such unstable modes are real and, indeed, their imaginary part is zero,  $\rho_\alpha = 0$  (see panel b)). One should thus expect the system to settle into stationary patterns, but that is not the case (panel c)); in fact, after a transient time, during which the solutions "seem to stabilise", they start to oscillate, in phase but about different average values.

To the best of our knowledge this is a novel oscillatory pattern that should be taken into account in the problem of patterns prediction [36]. Indeed, since the seminal paper by A. Turing [4], scholars are aware of the existence of stationary Turing patterns, often associated to a real dispersion relation, and of oscillatory Turing patterns resulting from a Turing wave instability. The use of discrete substrates such as networks questioned this dichotomy and a rule of thumb seems to apply [37]: oscillatory patterns develop if the most unstable mode has a large imaginary part,  $\rho_\alpha \gg \lambda_\alpha$ . The last example goes in the opposite direction because here  $\lambda_\alpha > \rho_\alpha = 0$  recalling that the final patterns is initiated by the linear behaviour, but rather shaped by the nonlinear character of the system.

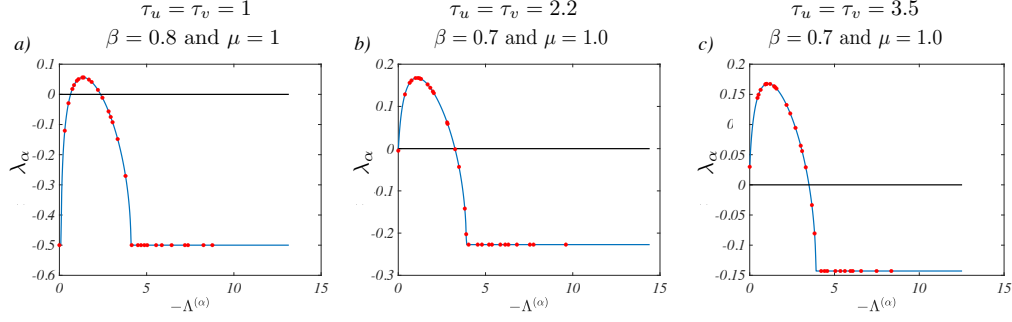


FIG. 3: **Dispersion relation for the *FHN* model,  $\tau_u = \tau_v$ .** For a fixed value of  $\gamma = 4$  and several couples  $(\beta, \mu)$  we show the dispersion relation,  $\lambda_\alpha$  as a function of  $\Lambda^{(\alpha)}$ . Panel a) corresponds to the choice  $\tau_u = \tau_v = 1$  and  $(\beta, \mu) = (0.8, 1.0)$  (yellow star in the panel c) of Fig. 2), lying the Turing instability region and indeed the dispersion relation assumes positive values. The homogeneous equilibrium is stable (the relation dispersion is negative for  $\Lambda^{(1)} = 0$ ), but it turns out to be unstable under heterogeneous perturbations and synchronised oscillatory patterns emerge (data not shown). In panel b) we fix  $\tau_u = \tau_v = 2.2$  and  $(\beta, \mu) = (0.7, 1.0)$  (red triangle in the panel c) of Fig. 2), still in the Turing region but conditioned to the value of  $\tau_{max}$ . The behaviour is similar to the one reported in panel a) but now the homogeneous equilibrium is weakly stable, the relation dispersion is negative but very close to 0 for  $\Lambda^{(1)} = 0$ , indeed for these values of the parameters we have  $\tau_{max} \sim 2.31$ . In panel c) we used the same parameters  $(\beta, \mu)$  but we increased  $\tau_u = \tau_v = 3.5 > \tau_{max}$  and indeed the homogeneous equilibrium is unstable, the dispersion relation is positive for  $\Lambda^{(1)} = 0$ . Again synchronised oscillatory patterns emerge (data not shown), they are indistinguishable from the ones one could obtain with the parameters used in panels a) and b) but they are not the result of Turing instability.

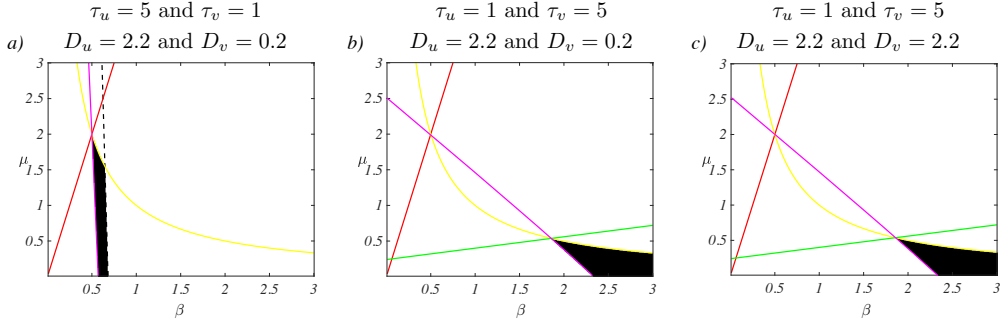


FIG. 4: **Parameters region associated to the inertia-driven Turing instability for the *FHN* model.** For a fixed value of  $\gamma = 4$ , we study the onset of Turing instability (black regions) close to the homogeneous equilibrium  $(u_i, v_i) = (0, 0)$ ,  $i = 1, \dots, n$ , as a function of  $\beta$  and  $\mu$  and driven by the inertial times,  $\tau_u \neq \tau_v$ . Indeed we assume  $D_u \geq D_v$ , resulting in a setting where classical Turing instability cannot emerge. Panel a) corresponds to the setting,  $\tau_u = 5$  and  $\tau_v = 1$ ,  $D_u = 2.2$  and  $D_v = 0.2$ . In panel b) we use the same diffusivities while the inertial times are exchanged, i.e.,  $\tau_u = 1$  and  $\tau_v = 5$ . Panel c) reports result for  $D_u = D_v = 2.2$  and  $\tau_u = 1$  and  $\tau_v = 5$ . In all the panels the red line denotes the condition  $\text{tr}(J_0) = 0$ , while  $\det(J_0) = 0$  is represented by the yellow one. The green line represents condition (19), while the magenta one represents condition (20); once present, the dashed black line stands for Eq. (23).

## V. DISCUSSION

In this work we have improved the Cattaneo framework of relativistic reaction-diffusion systems to allow for complex network substrates. We have thus analytically studied the conditions for the emergence of Turing instability for hyperbolic reaction-diffusion networked systems. The introduction of the inertial time removes the unphysical assumption of infinite propagation velocity, allowing thus to reduce the gap between experiment and theory. Indeed in this new framework, Turing instability emerges also for a setting where classical Turing instability cannot set, e.g., once the activator diffuses faster than the inhibitor.

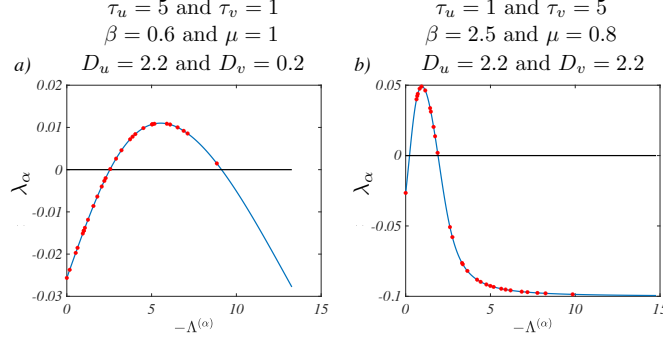


FIG. 5: **Dispersion relation for the *FHN* model in the case  $\tau_u \neq \tau_v$ .** For a fixed value of  $\gamma = 4$  and several couples  $(\beta, \mu)$  we show the dispersion relation,  $\lambda_\alpha$  as a function  $\Lambda^{(\alpha)}$ . Panel a) corresponds to the choice  $\tau_u = 5$  and  $\tau_v = 1$ ,  $(\beta, \mu) = (0.6, 1.0)$ , and  $D_u = 2.2$  and  $D_v = 0.2$ , lying in the inertia-driven Turing instability region (see panel a) Fig. 4). The aspatial equilibrium is stable ( $\lambda_1 < 0$ ), but it turns out to be unstable under heterogeneous perturbations and synchronised oscillatory patterns emerge (data not shown). In panel b), we fix  $\tau_u = 1$  and  $\tau_v = 5$ ,  $(\beta, \mu) = (0.7, 1.0)$ , still in the inertia-driven Turing region (see panel c) Fig. 4). The aspatial equilibrium is stable ( $\lambda_1 < 0$ ), but it turns out to be unstable under heterogeneous perturbations and synchronised oscillatory patterns emerge (data not shown).

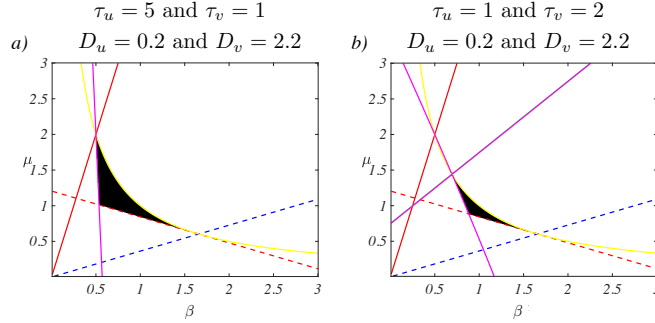


FIG. 6: **Parameters region associated to Turing instability for the *FHN* model,  $D_u < D_v$ .** For a fixed value of  $\gamma = 4$ , we study the onset of Turing instability (black regions) close to the homogeneous equilibrium  $(u_i, v_i) = (0, 0)$ ,  $i = 1, \dots, n$ , as a function of  $\beta$  and  $\mu$  and different choices of inertial times,  $\tau_u$  and  $\tau_v$ , and of the diffusivities,  $D_u$  and  $D_v$ , in a setting where classical Turing instability could emerge because  $D_u < D_v$ . Panel a) corresponds to the setting,  $\tau_u = 5$  and  $\tau_v = 1$ ,  $D_u = 0.2$  and  $D_v = 2.2$ , while panel b) shows results with the same diffusivities but  $\tau_u = 1$  and  $\tau_v = 2$ . In all the panels the red line denotes the condition  $\text{tr}(J_0) = 0$ , while  $\det(J_0) = 0$  is represented by the yellow one. The magenta line denotes the condition (20). The dashed blue line represents the condition  $D_v \partial_u f + D_u \partial_v g = 0$  (Eq. (24)), while the dashed red line the condition  $(D_u \partial_v g + D_v \partial_u f)^2 - 4 D_u D_v \det(J_0) = 0$  (Eq. (25)).

We have shown that the stability of the homogeneous solution is conditional to the inertial time common to both species. There exists a threshold,  $\tau_{max}$ , that, if exceeded, returns an unstable homogeneous solution: the system exhibits patterns but they are not ascribed to a Turing instability, let us observe that the latter are indistinguishable from the ones emerging following the Turing mechanism. Interestingly enough, such threshold depends on the model parameters and it can become arbitrarily large for a specific range of the latter; in such case, the homogeneous equilibrium is always stable (with respect to the inertial time). For generic values of the inertial times,  $\tau_u \neq \tau_v$ , we have proved that Turing instability can set up both for the inhibitor diffusing faster than the activator,  $D_v > D_u$ , as it occurs in the classical setting, but also in the complementary regime, i.e.,  $D_v \leq D_u$ , which is forbidden in the absence of inertial time.

We have complement our general analytical results with a numerical study of the FitzHugh-Nagumo model extended to the framework of hyperbolic reaction-diffusion networked systems. We have found stationary patterns as well as synchronised oscillatory ones; we have also found a new interesting class of solutions where the system spends a transient time into a stationary-like regime but then it evolves into an oscillatory one. This example raises relevant

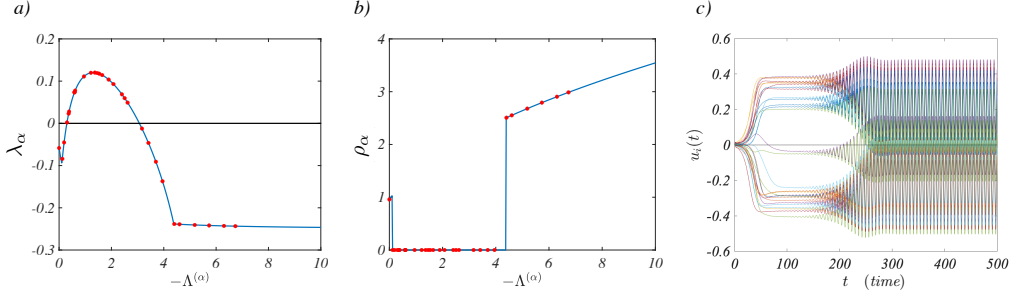


FIG. 7: **Dispersion relation and pattern for the *FHN* model**,  $\tau_u \neq \tau_v$ . For a fixed value of  $\gamma = 4$  and a choice of parameters corresponding to Turing instability (see panel b) Fig. 6),  $\tau_u = 1$ ,  $\tau_v = 2$ ,  $\beta = 0.9$ ,  $\mu = 1.0$ ,  $D_u = 0.2$  and  $D_v$ , we show in panel a) the dispersion relation, namely the  $\lambda_\alpha$  as a function  $\Lambda^{(\alpha)}$ . Panel b) corresponds to the imaginary part of the dispersion relation; we can appreciate the fact that the values associated to a positive  $\lambda_\alpha$  do have a zero imaginary part, while the decaying modes, i.e.,  $\lambda_\alpha < 0$ , are complex. This results into a novel pattern (panel c)) where the homogeneous solution turns out to be unstable, driven by the unstable modes  $\lambda_\alpha > 0$ , but the solution keeps oscillating (after a transient time) and does not settle onto a stationary pattern.

questions about the prediction of the patterns following a Turing instability, which is, up to now, an open problem [36].

The investigation discussed in this paper could be further extended in several directions. Previous studies have shown that different kinds of networks, such as directed [14] or non-normal ones [38, 39], extend the conditions for the emergence of patterns and allow for a richer spectrum of instabilities. Moreover, it has been shown that an instability similar to the Turing mechanism can be obtained by perturbing a stable limit cycle [40] and that non-normal networks further enhance such instability [41]. Given the oscillatory behaviours of neurones [23, 24] and the non-normal nature of neural networks [38], an extension towards such direction would open the way to interesting new results and applications.

### Acknowledgements

The authors are grateful to Duccio Fanelli and Anthony Hastir for useful comments and discussions. R.M. is supported by a FRIA-FNRS PhD fellowship, grant FC 33443, funded by the Walloon region.

### Appendix A: The Routh-Hurwitz criterion

The Routh-Hurwitz criterion [21, 32, 33] is a well known tool of dynamical systems and control theory, allowing to prove the linear (in)stability of an equilibrium for a time invariant system. Indeed, the latter relies on the spectral properties of the Jacobian matrix evaluated at the sought equilibrium, which ultimately accounts to determine the location in the complex plane of the roots of a suitable polynomial.

We hereby present the method using a fourth order polynomial, but it applies to any given order ones. Let thus  $p(\lambda) = a\lambda^4 + b\lambda^3 + c\lambda^2 + d\lambda + e$  be a polynomial with real coefficients and assume  $a > 0$ ; the Routh-Hurwitz criterion can be stated using the Hurwitz matrix associated to  $p(\lambda)$  and then compute its leading principal minors or building the Routh-Hurwitz table and check the signs of the first column.

More precisely, a necessary condition for the roots of  $p(\lambda)$  to have negative real part is that all the coefficients are positive:

$$a > 0, b > 0, c > 0, d > 0 \text{ and } e > 0, \quad (\text{A1})$$

while a sufficient condition is

$$a > 0, b > 0, bc - da > 0, d(bc - da) - eb^2 > 0 \text{ and } e > 0. \quad (\text{A2})$$

## 1. Application of the criterion to the stability of $p_1(\lambda)$

Let us now apply the Routh-Hurwitz criterion to determine the stability feature of the polynomial  $p_1(\lambda)$  given by Eq. (11), hereby rewritten

$$\begin{aligned} p_1(\lambda) &= a\lambda^4 + b\lambda^3 + c_1\lambda^2 + d_1\lambda + e_1 \\ &= \tau_u\tau_v\lambda^4 + (\tau_u + \tau_v)\lambda^3 + [1 - \tau_u\partial_v g - \tau_v\partial_u f]\lambda^2 + [-\text{tr}(J_0)]\lambda + \det(J_0). \end{aligned}$$

Being the coefficients of  $a = \tau_u\tau_v$  and  $b = \tau_u + \tau_v$  positive, the Routh-Hurwitz criterion rewrites:

$$c_1 > 0, d_1 > 0, bc_1 - d_1a > 0, d_1(bc_1 - d_1a) - b^2e_1 > 0 \text{ and } e_1 > 0.$$

Replacing the definition of the coefficients in the above equation, we straightforwardly obtain the five conditions (16)–(20).

## 2. Application of the criterion to the stability of $p_\alpha(\lambda)$

Let us now study the instability character of  $p_\alpha(\lambda)$ , for some  $\alpha > 1$  under the assumption of stability for  $p_1(\lambda)$ . We once again rely on the Routh-Hurwitz criterion. Let us thus rewrite

$$p_\alpha(\lambda) = a\lambda^4 + b\lambda^3 + c_\alpha\lambda^2 + d_\alpha\lambda + e_\alpha,$$

where again  $a = \tau_u\tau_v$ ,  $b = \tau_u + \tau_v$  and

$$\begin{aligned} c_\alpha &= 1 - \tau_u\partial_v g - \tau_v\partial_u f - \Lambda^{(\alpha)}(\tau_u D_v + \tau_v D_u) = c_1 - \Lambda^{(\alpha)}(\tau_u D_v + \tau_v D_u) \\ d_\alpha &= -\text{tr}(J_0) - \Lambda^{(\alpha)}(D_v + D_u) = d_1 - \Lambda^{(\alpha)}(D_v + D_u) \\ e_\alpha &= \det(J_0) + (D_v\partial_u f + D_u\partial_v g)\Lambda^{(\alpha)} + D_u D_v \left(\Lambda^{(\alpha)}\right)^2, \end{aligned}$$

where we emphasised the relation between the coefficients defined for  $\alpha > 1$  and those for  $\alpha = 1$ .

As already observed, the coefficients  $a$  and  $b$  are positive. Moreover, because of the assumption on the stability of  $p_1(\lambda)$ , we also have  $c_1 > 0$  and  $d_1 > 0$ . Finally, observing that  $-\Lambda^{(\alpha)} \geq 0$  for all  $\alpha$  we can conclude that

$$c_\alpha > 0 \text{ and } d_\alpha > 0 \quad \forall \alpha.$$

The Routh-Hurwitz criterion ensures that  $p_1(\lambda)$  is unstable if at least one of the following conditions is met:

- i)  $bc_\alpha - d_\alpha a < 0$ ;
- ii)  $d_\alpha(bc_\alpha - d_\alpha a) - b^2e_\alpha < 0$ ;
- iii)  $e_\alpha < 0$ .

Let us first show that condition i) is never met under the assumption of stability of  $p_1(\lambda)$ . From the definitions of the coefficients  $a$ ,  $b$ ,  $c_\alpha$  and  $d_\alpha$  we obtain

$$\begin{aligned} bc_\alpha - d_\alpha a &= (\tau_u + \tau_v) \left[ c_1 - \Lambda^{(\alpha)}(\tau_u D_v + \tau_v D_u) \right] - \tau_u\tau_v \left[ d_1 - \Lambda^{(\alpha)}(D_v + D_u) \right] \\ &= (\tau_u + \tau_v)c_1 - \tau_u\tau_v d_1 - \Lambda^{(\alpha)}[(\tau_u + \tau_v)(\tau_u D_v + \tau_v D_u) - \tau_u\tau_v(D_v + D_u)] \\ &= bc_1 - d_1a - \Lambda^{(\alpha)}(\tau_u^2 D_v + \tau_v^2 D_u). \end{aligned}$$

We can now conclude that  $bc_\alpha - d_\alpha a > 0$ ; indeed because of the stability of  $p_1(\lambda)$ ,  $bc_1 - d_1a > 0$ , and being  $-\Lambda^{(\alpha)} > 0$  for all  $\alpha > 1$ , the claim easily follows.

Let us now consider condition ii) and look for the existence of  $\alpha > 1$  such that

$$d_\alpha(bc_\alpha - d_\alpha a) - b^2e_\alpha < 0.$$

We firstly rewrite this equation by using the definition of the involved coefficients

$$\begin{aligned} & (d_1 - \Lambda^{(\alpha)}(D_v + D_u)) \left[ (\tau_u + \tau_v)(c_1 - \Lambda^{(\alpha)}(\tau_u D_v + \tau_v D_u)) - (\tau_u\tau_v)(d_1 - \Lambda^{(\alpha)}(D_v + D_u)) \right] + \\ & - (\tau_u + \tau_v)^2 \left[ \det(J_0) + (D_v\partial_u f + D_u\partial_v g)\Lambda^{(\alpha)} + D_u D_v (\Lambda^{(\alpha)})^2 \right] < 0 \end{aligned},$$

and then we reorganise the terms in the latter, to write it as a second order polynomial in the variable  $\Lambda^{(\alpha)}$ , hence:

$$A \left( \Lambda^{(\alpha)} \right)^2 + B \Lambda^{(\alpha)} + C < 0,$$

where (after some algebraic manipulation):

$$\begin{aligned} A &= (\tau_u D_v - \tau_v D_u)^2 \\ B &= -(\tau_u + \tau_v)(D_u + D_v)(1 - \tau_u \partial_v g - \tau_v \partial_u f) + (\tau_u + \tau_v) \text{tr}(J_0)(\tau_u D_v + \tau_v D_u) \\ &\quad - 2 \text{tr}(J_0)(D_u + D_v) \tau_u \tau_v - (\tau_u + \tau_v)^2 (D_v \partial_u f + D_u \partial_v g) \\ C &= d_1(bc_1 - ad_1) - b^2 e_1. \end{aligned}$$

The coefficient  $A$  is positive, as well as the coefficient  $C$ , under the assumption of stability for  $p_1(\lambda)$ . Then the second order polynomial in  $\Lambda^{(\alpha)}$  can exhibit negative values if and only if

$$B > 0 \text{ and } B^2 - 4AC > 0,$$

that are exactly the conditions (22) and (23). Finally, an eigenvalue  $\Lambda^{(\bar{\alpha})}$ ,  $\bar{\alpha} > 1$ , must exist such that

$$x_1 < \Lambda^{(\bar{\alpha})} < x_2,$$

where  $x_1$  and  $x_2$  are the two real and negative roots of second order polynomial in  $\Lambda^{(\alpha)}$ .

Let us finally consider condition iii) and look for the existence of  $\alpha > 1$  such that

$$e_\alpha = \det(J_0) + (D_v \partial_u f + D_u \partial_v g) \Lambda^{(\alpha)} + D_u D_v \left( \Lambda^{(\alpha)} \right)^2 < 0.$$

This is a second order polynomial in the variable  $\Lambda^{(\alpha)}$  whose leading coefficient,  $D_u D_v$ , is positive as well as the constant term,  $\det(J_0)$ , because of the stability of  $p_1(\lambda)$ . The polynomial can thus assume negative values if and only if

$$\begin{aligned} D_v \partial_u f + D_u \partial_v g &> 0 \\ (D_v \partial_u f + D_u \partial_v g)^2 - 4 D_u D_v \det(J_0) &> 0. \end{aligned}$$

Namely, the conditions (24) and (25). Let us observe that the latter do not depend on  $\tau_u$  and  $\tau_v$  and indeed they are the classical conditions required for the Turing instability to arise [13]: an eigenvalue  $\Lambda^{(\bar{\alpha})}$ ,  $\bar{\alpha} > 1$ , must exist such that

$$\eta_1 < \Lambda^{(\bar{\alpha})} < \eta_2,$$

where  $\eta_1$  and  $\eta_2$  are the two real and negative roots of  $e_\alpha = 0$ .

- 
- [1] Nicolis G, Prigogine I. 1977 Self-organization in nonequilibrium systems: From dissipative structures to order through fluctuations. J.Wiley and Sons.
  - [2] Murray JD. 2001 Mathematical biology II: Spatial models and biomedical applications. Springer- Verlag.
  - [3] Pastor-Satorras R, Vespignani A. 2010 Patterns of complexity. Nature Physics 6, 480.
  - [4] Turing AM. 1952 The chemical basis of morphogenesis. Phil. Trans. R. Soc. Lond. B 237, 37.
  - [5] Pecora LM, Carroll TL, Johnson GA, Mar DJ, Heagy JF. 1997 Fundamentals of synchronization in chaotic systems, concepts, and applications. Chaos: An Interdisciplinary Journal of Nonlinear Science 7, 520–543.
  - [6] Strogatz SH. 2001 Exploring complex networks. Nature 410, 268.
  - [7] Pismen LM. 2006 Patterns and interfaces in dissipative dynamics. Springer Science & Business Media.
  - [8] Gierer A, Meinhardt H. 1972 A theory of biological pattern formation. Kybernetik 12, 30.
  - [9] Crampin E, Gaffney E, Maini P. 1999 Reaction and diffusion on growing domains: scenarios for robust pattern formation. Bull. Math. Biol. 61, 1093.
  - [10] Plaza R, Sánchez-Garduño F, Padilla P, Barrio R, Maini P. 2004 The effect of growth and curvature on pattern formation. J. Dyn. Differ. Equ. 16, 1093.

- [11] Van Gorder R. 2020 Turing and Benjamin-Feir instability mechanisms in non-autonomous systems. *Proceedings of the Royal Society A* 476, 20200003.
- [12] Othmer HG, Scriven L. 1974 Non-linear aspects of dynamic pattern in cellular networks. *Journal of Theoretical Biology* 43, 83–112.
- [13] Nakao H, Mikhailov AS. 2010 Turing patterns in network-organized activator-inhibitor systems. *Nature Physics* 6, 544.
- [14] Asllani M, Challenger JD, Pavone FS, Sacconi L, Fanelli D. 2014a The theory of pattern formation on directed networks. *Nature Communications* 5, 4517.
- [15] Asllani M, Busiello D, Carletti T, Fanelli D, Planchon G. 2014b Turing patterns in multiplex networks. *Physical Review E* 90, 042814.
- [16] Petit J, Lauwens B, Fanelli D, Carletti T. 2017 Theory of Turing Patterns on Time Varying Networks. *Phys. Rev. Letters* 119, 148301.
- [17] Van Gorder R. 2021 A theory of pattern formation for reaction-diffusion systems on temporal networks. *Proceedings of the Royal Society A* 477, 20200753.
- [18] Cattaneo G 1948 Sulla conduzione del calore. *Atti. Sem. Mat. Fis. Univ. Modena* p. 83.
- [19] Casas-Vázquez J, Jou D, Lebon G. 1996 *Extended Irreversible Thermodynamics*. Springer, Berlin.
- [20] Zemskov EP, Horsthemke W. 2016 Diffusive instabilities in hyperbolic reaction-diffusion equations. *Physical Review E* 93, 032211.
- [21] Hurwitz A. 1895 Ueber die Bedingungen, unter welchen eine Gleichung nur Wurzeln mit negativen reellen Theilen besitzt. *Math. Ann.* 46, 273.
- [22] Currò A, Valenti G. 2021 Pattern formation in hyperbolic models with cross-diffusion: Theory and applications. *Physica D* 418, 132846.
- [23] FitzHugh R. 1961 Impulses and physiological states in theoretical models of nerve membrane. *Biophys. J.* 1, 445.
- [24] Nagumo J, Arimoto S, Yoshizawa S. 1962 An active pulse transmission line simulating nerve axon. *Proc. IRE* 50, 2061.
- [25] Rinzel J, Keller JB. 1973 Traveling wave solutions of a nerve conduction equation. *Biophys. J.* 13, 1313.
- [26] Ohta T. 1989 Decay of Metastable Rest State in Excitable Reaction-Diffusion System. *Prog. Theoret. Phys. Suppl.* 99, 425.
- [27] Shoji H, Yamada K, Ueyama D, Ohta T. 2007 Turing patterns in three dimensions. *Phys. Rev. E* 75, 046212.
- [28] Carletti T, Nakao H. 2020 Turing patterns in a network-reduced FitzHugh-Nagumo model. *Phys. Rev. E* 101, 022203.
- [29] Siebert B, Hall C, Gleeson J, Asllani M. 2020 Role of modularity in self-organization dynamics in biological networks. *Physical Review E* 102, 052306.
- [30] Vragovic I, Louis E, Díaz-Guilera A. 2006 Performance of excitable small-world networks of Bonhoeffer-van der Pol-FitzHugh-Nagumo oscillators. *Europhys. Lett.* 76, 780.
- [31] Aqil M, Hong KS, Jeong MY. 2012 Synchronization of coupled chaotic FitzHugh-Nagumo systems. *Communications in Nonlinear Science and Numerical Simulation* 17, 1615.
- [32] Routh EJ. 1877 *Stability of a given state of motion*. MacMillan and Co, London.
- [33] Barnett S. 1983 *Polynomials and Linear Control Systems*. Dekker, New York.
- [34] Strogatz S. 2014 *Nonlinear Dynamics and Chaos*. Avalon Publishing.
- [35] Erdős P, Rényi A. 1969 On the evolution of random graphs. *Publications of the Mathematical Institute of the Hungarian Academy of Sciences* 5, 17.
- [36] Subramanian S, Murray S. 2021 Pattern selection in reaction diffusion systems. *Phys. Rev. E* 103, 012215.
- [37] Asllani M, Carletti T, Fanelli D, Maini P. 2020 A universal route to pattern formation in multicellular systems. *The European Physical Journal B* 93, 1.
- [38] Asllani M, Lambiotte R, Carletti T. 2018 Structure and dynamics of non-normal networks. *Sci. Adv.* 4, Eaau9403.
- [39] Muolo R, Asllani M, Fanelli D, Maini P, Carletti T. 2019 Patterns of non-normality in networked systems. *Journal of Theoretical Biology* 480, 81.
- [40] Challenger J, Fanelli D, Burioni R. 2015 Turing-like instabilities from a limit cycle. *Phys. Rev. E* 92, 022818.
- [41] Muolo R, Carletti T, Gleeson J, Asllani M. 2021 Synchronization dynamics in non-normal networks: the trade-off for optimality. *Entropy* 23, 36.